Double folding cluster potential for $^{12}C+^{12}C$ elastic scattering

M. A. Hassanain,[1] Awad A. Ibraheem,[2] and M. El-Azab Farid[3]
[1]*Sciences Department, New-Valley Faculty of Education, Assiut University, El-Kharga, New-Valley, Egypt*
[2]*Physics Department, Al-Azhar University, Assiut 71524, Egypt*
[3]*Physics Department, Assiut University, Assiut 71516, Egypt*
(Received 13 October 2007; revised manuscript received 11 January 2008; published 7 March 2008)

Using the alpha (α)-cluster structure of ^{12}C nucleus, two versions of the $^{12}C+^{12}C$ real double folded optical potentials have been generated based upon effective α-α, α-nucleon (N) and N-N interactions. The obtained potentials, in conjunction with shallow phenomenological Woods-Saxon imaginary parts, successfully reproduce the elastic scattering differential cross section for 12 sets of data over the broad energy range 70–360 MeV. No renormalization of the real folded potentials is required to fit the data. The energy dependence of the extracted real and imaginary volume integrals and total reaction cross section is investigated.

DOI: 10.1103/PhysRevC.77.034601 PACS number(s): 21.60.Gx, 24.10.Ht, 24.50.+g, 25.70.Bc

I. INTRODUCTION

Knowledge of the ion-ion interaction potential is a key ingredient in the analysis of nuclear reactions. By using the potential between colliding nuclei we can estimate the cross sections of different nuclear reactions such as elastic, inelastic and fusion reactions, which are strongly dependent on the nucleus-nucleus interaction potential [1–3]. Although many different approaches to the nuclear part of the interaction potential have been adopted, this part is still, unfortunately, less defined.

In the last three decades, several attempts have been performed to develop folding formulations of the optical model potential for the analyses of the elastic and inelastic heavy ions (HI) scattering [4–13]. The original version of the double folding (DF) model [14] based upon a realistic effective nucleon-nucleon (NN) interaction successfully described most of scattering reactions dominated by the strong absorption, which makes the HI elastic scattering data sensitive only to the surface part of the nucleus-nucleus potential. However, the situation is different if a refractive or rainbow scattering is observed, where the data are sensitive to the nuclear potential over a wider radial domain. For such reactions the simple DF model [14] failed to give a good description of the data. Refractive scattering contribution in HI systems, such as $^{12}C+^{12}C$, $^{12}C+^{16}O$, $^{16}O+^{16}O$, has been discussed in several articles (e.g., Refs. [6,8,15–18]).

Some attempts [4,5] were carried out to impose on the M3Y effective NN interaction [19] an explicit density dependence to account effectively for the in-medium effects which are more substantial at internuclear distances, the so-called DDM3Y interaction. Khoa *et al.* [6] used, also, different density-dependent versions of the M3Y effective interaction for analyses of the elastic scattering of $^{12}C+^{12}C$, $^{16}O+^{16}O$ data.

On the other hand, El-Azab Farid *et al.* [8,9], and recently Karakoc and Boztosun [10], have employed the α-cluster structure of the interacting nuclei in the folding formalism to generate α-particle single folding cluster (SFC) and light HI double folding cluster (DFC) optical potentials based upon an appropriate α-α interaction. They [8,9] assumed that projectile and target nuclei consist of an integer multiple of the number of α-particles. However, in most of the studied reactions [8–10], it was essential to introduce reducing renormalization coefficients ($\sim$0.7–0.9) in order to obtain successful description of the HI elastic scattering data.

Recently, Abdullah *et al.*, in three successive articles [11–13], have proposed a SFC model to successfully reproduce the differential cross-section of elastic scattering of α-particles on ^{12}C,^{16}O and $^{40,44,48}Ca$ and $^{16}O+^{12}C$ over a broad spectrum of incident energies. In this model they [11–13] considered the view that most of the time a number of nucleons in the target nucleus are primarily in α-like clusters and the rest are in an unclustered nucleonic configuration. This leads to the folding potential as a sum of two potentials, one convoluted over the α-cluster density distribution and the other over the nucleonic density distribution. In this formalism no renormalization was required in order to fit the data. Furthermore, they [11–13] deduced the α-cluster structure configurations for ^{12}C, ^{16}O, and $^{40,44,48}Ca$, respectively as $2.35\alpha + 2.6N$, $3.5\alpha + 2N$, $8.5\alpha + 6N$, $8.5\alpha + 10N$, and $8.5\alpha + 14N$.

In the present study we investigate the $^{12}C+^{12}C$ elastic scattering in the framework of the two models, the DFC of El-Azab Farid *et al.* [8,9] and a DFC extended from the SFC of Abdullah *et al.* [11–13]. For the sake of comparison we construct both models based upon the same α-α interaction. Twelve sets of data are analyzed over the broad energy range 70–360 MeV using the generated DFC potentials. In the following section, a theoretical formalism is presented, while calculations procedure is described in Sec. III. Section IV is devoted for results and discussion and finally conclusions are summarized in Sec. V.

II. THEORETICAL FORMALISM

A. Folding approaches

Our aim in the present study is to describe the $^{12}C+^{12}C$ elastic scatting using two different semimicroscopic real folded potentials. In the first, the cluster structure $^{12}C \equiv 3\alpha$ is considered. Then, the folded potential, denoted as DFC1, is generated by folding an effective α-α interaction over the α-cluster density distributions in both projectile and target

nuclei [8,9]. In this context, if one denotes the density distributions of α-clusters inside the projectile and target nuclei by ρ_{CP} and ρ_{CT}, respectively, the DFC1 potential can be expressed as [8,9]

$$U_{\mathrm{DFC1}}(R) = \int\int \rho_{CP}(r_1)\rho_{CT}(r_2)V_{\alpha\text{-}\alpha}(|\vec{R} - \vec{r}_1 + \vec{r}_2|)d\vec{r}_1 d\vec{r}_2. \tag{1}$$

Here, R denotes the projectile-target relative position vector and r_1 and $r_2$are, respectively, the c.m. coordinates of the α-clusters in the projectile and target nuclei. The α-α effective interaction $V_{\alpha\text{-}\alpha}$ is parametrized as [11–13,20]

$$V_{\alpha\text{-}\alpha}(s) = V_R \exp\left(-\mu_R^2 s^2\right) - V_A \exp\left(-\mu_A^2 s^2\right), \tag{2}$$

where V_A and V_R are the attractive and repulsive depths and μ_A and μ_R are the corresponding range parameters. We consider $V_A = 122.62$ MeV, $\mu_A = 0.469$ fm^{-1}, and $\mu_R = 0.54$ fm^{-1}, while the depth V_R is kept free parameter in the calculations. The α-cluster distribution inside ^{12}C is described in the next subsection.

To deduce the second folded potential, denoted as DFC2, we consider the cluster structure $^{12}\mathrm{C} \equiv A_\alpha\alpha + A_N N$; i.e., ^{12}C nucleus is composed of A_α α-particles plus A_N unclustered nucleons, such that $4A_\alpha + A_N = 12$. Consequently, if one denotes the density distributions of the α-clusters and unclustered nucleons in the projectile and target by $\rho_{\alpha P}$, ρ_{NP}, $\rho_{\alpha T}$, and ρ_{NT}, respectively, the DFC2 potential can be constructed as

$$\begin{aligned} U_{\mathrm{DFC\ 2}}(R) = &\int\int \rho_{\alpha P}(r_{\alpha P})\rho_{\alpha T}(r_{\alpha T})V_{\alpha-\alpha}(|\vec{R} - \vec{r}_{\alpha P} + \vec{r}_{\alpha T}|)d\vec{r}_{\alpha P}d\vec{r}_{\alpha T} \\ &+ \int\int \rho_{\alpha P}(r_{\alpha P})\rho_{NT}(r_{NT})V_{\alpha-N}(|\vec{R} - \vec{r}_{\alpha P} + \vec{r}_{NT}|)d\vec{r}_{\alpha P}d\vec{r}_{NT} \\ &+ \int\int \rho_{\alpha T}(r_{\alpha T})\rho_{NP}(r_{NP})V_{\alpha-N}(|\vec{R} - \vec{r}_{\alpha T} + \vec{r}_{NP}|)d\vec{r}_{\alpha T}d\vec{r}_{NP} \\ &+ \int\int \rho_{NT}(r_{NT})\rho_{NP}(r_{NP})V_{N-N}(|\vec{R} - \vec{r}_{NT} + \vec{r}_{NP}|)d\vec{r}_{NT}d\vec{r}_{NP}, \end{aligned} \tag{3}$$

where $\mathrm{r}_{\alpha P}(r_{NP})$ and $r_{\alpha T}(r_{NT})$ are, respectively, the c.m. coordinates of the α-clusters (unclustered nucleons) in the projectile and target nuclei, $V_{\alpha-N}$ and V_{N-N} are the α-N and NN effective interactions, respectively. The α–N interaction has the following form [21]:

$$V_{\alpha-N}(s) = -V_{0\alpha N}\exp(-K^2 s^2), \tag{4}$$

where $V_{0\alpha N} = 47.3$ MeV and $K = 0.435$ fm^{-1}. The NN potential is given in a Gaussain form as [7,22]

$$V_{N-N}(s) = -V_{0NN}\exp\left[-\left(\frac{s}{a}\right)^2\right] \tag{5}$$

with $V_{0NN} = 20.97$ MeV and $a = 1.47$ fm.

B. Density distributions

We consider, first, the cluster structure $^{12}\mathrm{C} \equiv 3\alpha$. The matter density of ^{12}C nucleus is usually expressed in a modified form of the Gaussian shape as [8]

$$\rho_m(r) = \rho_{0m}(1 + wr^2)\exp(-\beta r^2). \tag{6}$$

The matter density of the α-particle can also be obtained by the Gaussian form as [9,14]

$$\rho_\alpha(r) = \rho_{0\alpha}\exp(-\lambda r^2). \tag{7}$$

The parameters$\rho_{0(m,\alpha)}$, ρ_{0M}, ω, β, and λ and the corresponding root mean square (rms) radii are given in Table I.

Now, if $\rho_C(r')$ is the α-cluster distribution function inside ^{12}C nucleus, then we can relate the nuclear matter density distribution functions (6) and (7) as [8]

$$\rho_m(r) = \int \rho_C(r')\rho_\alpha(|\vec{r} - \vec{r}'|)d\vec{r}'. \tag{8}$$

Then, using Fourier transform techniques [14] for expression (8), we can obtain

$$\rho_C(r') = \rho_{0C}(1 + \gamma r'^2)\exp(-\xi r'^2), \tag{9}$$

where

$$\xi = \frac{\beta\lambda}{\eta}, \quad \eta = \lambda - \beta \quad \text{and} \quad \gamma = \frac{2\omega\lambda^2}{[\eta(2\eta - 3\omega)]}.$$

The parametersρ_{0C}, γ and ξ used in Eq. (9) are, also, listed in Table I. It is evident form this table that the values for the α-cluster density in ^{12}C nucleus are negative near the origin, i.e., at $r \leqslant 0.7$ fm. One can notice [23] from Eq. (8) and using the Fourier transform in the momentum space q, that the carbon form factor should have a zero whenever the α-particle does. Now the free α-particle form factor has such

TABLE I. Density parameters used in Eqs. (6), (7), and (9) and the corresponding rms radii [8].

Nucleus	$\rho_{0(m,\alpha,C)}$ (fm^{-3})	$\omega(\gamma)$ (fm^{-2})	$\beta(\lambda)(\xi)$ (fm^{-2})	rms radius (fm)
$\rho_m(r)$	0.1644	0.4988	0.3741	2.407
$\rho_\alpha(r)$	0.4229	0	0.7024	1.460
$\rho_C(r)$	−0.1644	−1.7852	0.8003	1.912

a zero for $q^2 \cong 10$ fm^{-2}, whereas there is no sign of such out to the limit of carbon measurement ($q^2 \cong 11$ fm^{-2}). Inopin and Tishchenko [24] suggested that perhaps the size of the α-particle is slightly changed inside the nucleus, and that the zero is displaced to just outside the measured region. This may be cured by involving a correction term depends on the rms radius of the α-particle inside the nucleus. On the other side, owing to the small number of α-clusters inside ^{12}C nucleus which are distributed over the surface in an equilateral triangle configuration, it is not expected to find α-clusters close to the center of the nucleus, such that this problem disappeared for the other nuclei when the number of α-clusters increased [23]. The negative density discrepancy was also obtained previously during the analysis of pion-carbon elastic scattering data using the 3α-cluster model for the structure of ^{12}C nucleus [25].

Now we assume the approach for the cluster structure of ^{12}C as $^{12}\text{C} \equiv A_\alpha \alpha + A_N N$. The density distributions of the α-clusters and unclustered nucleons in ^{12}C are taken to be of the modified Gaussain form as [13]

$$\rho_{iC}(r) = \rho_{0i}(1 + wr^2)\exp(-\beta_i r^2) \tag{10}$$

where $i = \alpha, N$. Since ^{12}C nucleus is composed of A_α α-particles plus A_N unclustered nucleons, then we have the normalization integral as

$$\int \rho_{\alpha C}(r)d\vec{r} + \int \rho_{NC}(r)d\vec{r} = 4A_\alpha + A_N = 12. \tag{11}$$

The considered values of the parameters are as follows [13]: $\rho_{0\alpha} = 0.0336$ fm^{-3}, $\rho_{0N} = 0.2186$ fm^{-3}, $w = 0.496$ fm^{-2}, $\beta_\alpha = 0.381$ fm^{-2}, and $\beta_N = 0.9$ fm^{-2}. These values yield $A_\alpha = 2.35$ and $A_N = 2.6$ and the corresponding rms radius of ^{12}C equals 2.46 fm. These parameters were recently [13] used to successfully describe the α+^{12}C and ^{16}O+^{12}C elastic scattering over the energy range 29–172 MeV. Finally, we can derive the DFC2 potential (3) using the density distributions (10) together with the α-α, α-N, and NN interactions defined by Eqs. (2), (4), and (5), respectively.

III. PROCEDURE

The semimicroscopic potentials, DFC1 and DFC2 generated from Eqs. (1) and (3) are considered as the real part of the ^{12}C+^{12}C optical potential. The imaginary part is taken in the phenomenological Woods-Saxon (WS) shape as

$$W(R) = -W_0 \Big/ \left[1 + \exp\left(\frac{R - R_I}{a_I}\right)\right], \quad R_I = 2r_I x 12^{1/3}, \tag{12}$$

where W_0, r_I, and a_I are the depth, radius, and diffuseness parameters. Then, the nucleus-nucleus interaction may be written in the form

$$U(R) = U_{\text{DFC1(DFC2)}}(R) + iW(R) + V_C(R), \tag{13}$$

where V_C is the repulsive Coulomb potential, which is represented by the interaction between two uniform charge distributions of radius parameter equals 1.25 fm.

The obtained potentials are fed into the computer code HI-OPTIM-94 [26] to calculate the elastic scattering differential cross sections. To obtain the best fit between the experimental data and the theoretical calculations, we have conducted a $\chi 2$ search to define the parameters of the potentials. The $\chi 2$ value is defined as

$$\chi^2 = \frac{1}{N_D}\sum_{k=1}^{N_D}\left[\frac{\sigma_{\text{th}}(\theta_k) - \sigma_{\text{exp}}(\theta_k)}{\Delta\sigma_{\text{exp}}(\theta_k)}\right]^2 \tag{14}$$

where N_D is the number of differential cross-section data points, $\sigma_{\text{th}}(\theta_k)$ is the calculated cross section at angle θ_k in the c.m. system, $\sigma_{\text{exp}}(\theta_k)$ and $\Delta\sigma_{\text{exp}}(\theta_k)$ are the corresponding experimental cross section and its relative uncertainty, respectively. All potential parameters are held constant during the search except the depth of the real repulsive part of α-α interaction, V_R, and the depth of the imaginary potential, W_0, where they are freely adjusted in order to obtain best fits to data.

IV. RESULTS AND DISCUSSION

In the present work, 12 sets of data for the differential cross section of ^{12}C+^{12}C elastic scattering at energies from 70.7 to 360 MeV are analyzed using the generated DFC1 and DFC2 potentials. The obtained parameters and associated real and imaginary volume integrals per interacting nucleon-pair, J_R, J_I, in addition to the resulted reaction cross sections, σ_R, are listed in Table II and the corresponding fits with experimental data are shown in Figs. 1–3.

From these figures, it is clear that, in general, successful descriptions of the data are obtained using both of the DFC1 and DFC2 potentials. Only two exceptions are observed for 89.7 and 300 MeV energies at backward angles, where theoretical underestimation is found. From this comparison one may, also, notice that introducing the treatment of unclustered nucleons in the structure of ^{12}C through the DFC2 potential relatively reduces the amplitude of oscillation, which

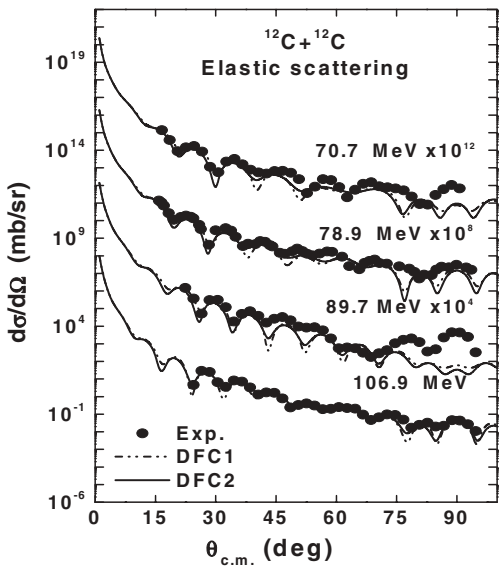

FIG. 1. A comparison between the measured ^{12}C+^{12}C elastic scattering differential cross sections and theoretical predictions obtained using the DFC1 and DFC2 potentials at energies of 70.7, 78.9, 89.8, and 106.9 MeV. Data are taken from [27].

TABLE II. Best-fit parameters obtained for the DFC1 and DFC2 potentials analysis of $^{12}C+^{12}C$ elastic scattering. The parameters $r_I = 1.23$ fm and $a_I = 0.505$ fm are kept fixed during the search.

Potential	Energy (MeV)	V_R (MeV)	W_0 (MeV)	J_R (MeV fm^3)	J_I (MeV fm^3)	σ_R (mb)	χ^2
DFC1	70.7	33.0	11.0	340.7	61.6	1259	36.6
DFC2		166.0	11.2	286.8	62.7	1280	35.8
DFC1	78.9	28.0	12.3	351.7	68.5	1285	28.3
DFC2		156.0	12.4	300.4	69.7	1308	30.0
DFC1	89.7	28.0	22.7	353.9	115.8	1373	53.2
DFC2		152.0	21.5	305.0	120.6	1402	54.3
DFC1	106.9	28.0	13.8	349.5	85.9	1334	10.9
DFC2		167.0	13.5	285.5	75.9	1321	10.3
DFC1	112.0	30.0	14.4	347.3	91.0	1344	17.5
DFC2		168.0	14.2	284.1	79.4	1328	11.0
DFC1	117.1	30.0	14.1	347.3	88.0	1339	13.4
DFC2		188.0	13.8	267.8	77.2	1316	12.3
DFC1	121.6	31.0	15.3	345.1	95.7	1353	15.2
DFC2		172.0	15.3	278.7	85.5	1338	17.8
DFC1	126.7	35.0	15.0	336.2	98.0	1356	17.8
DFC2		182.0	14.7	265.0	82.7	1326	12.4
DFC1	158.9	37.0	17.8	331.8	113.8	1380	47.7
DFC2		164.0	18.6	289.5	104.2	1371	25.9
DFC1	300.0	76.0	18.1	245.6	107.7	1321	22.8
DFC2		198.0	19.4	243.4	108.8	1325	23.9
DFC1	344.0	76.0	13.6	245.6	76.6	1225	9.6
DFC2		198.0	11.8	243.4	66.0	1185	8.1
DFC1	360.0	90.0	14.9	219.1	90.0	1257	24.2
DFC2		232.0	15.3	197.4	85.6	1240	13.2

yields slight improvement in the fitting with data, particularly at forward angles.

On the other hand, it is observable that, at the lower considered energies, predictions produced by the DFC2 potential are more successful than those produced by the DFC1 one. At the three highest energies (300, 344, and 360 MeV) the situation seems to be reversed, where predictions of the DFC1 potential are the best. This may indicate that the number of unclustered nucleons decreases when energy of

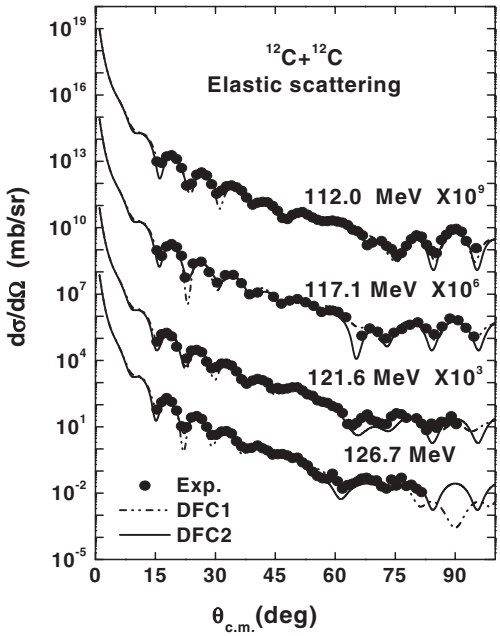

FIG. 2. Same as Fig. 1, but at energies of 112, 117.1, 121.6, and 126.7 MeV. Data are taken from [27].

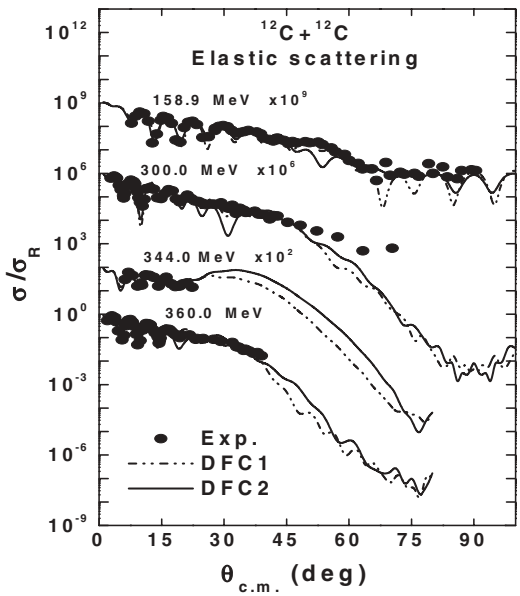

FIG. 3. Same as Fig. 1 but at energies of 158.9, 300, 344, and 360 MeV. Data are taken from [15].

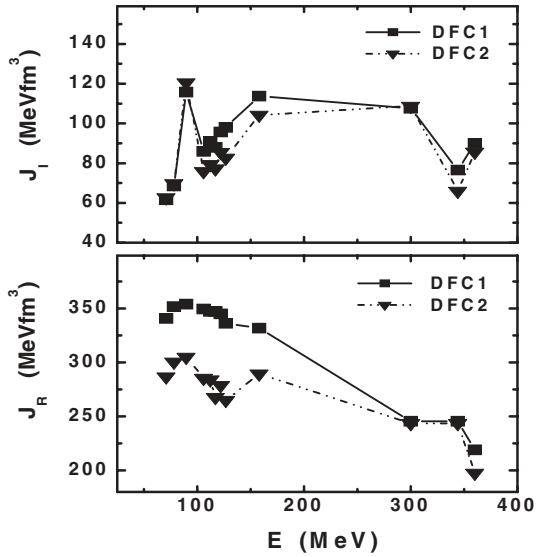

FIG. 4. Energy dependence of the real and imaginary volume integrals of the DFC1, DFC2 and imaginary WS potentials. Lines are drawn to guide eyes.

^{12}C projectiles increases, consequently, full α-clustering in ^{12}C nucleus ($A_\alpha = 3$, $A_N = 0$) dominates at higher energies.

The obtained values of real and volume integrals, noted in Table II, are plotted against energy as shown in Fig. 4. It is clear that at low energies the real volume integrals, J_R, of the DFC1 are significantly larger than those of the DFC2 one. This behavior results from the values of the repulsive depth, V_R, used in the calculations, where $V_R(\text{DFC2})/V_R(\text{DFC2}) > 5$, while at the higher energies this factor reduces to about 2 and J_R values of both potentials are almost similar. On the other side, the obtained values of J_R are significantly larger than those found [13] from the analysis of the refractive ^{16}O+^{12}C elastic scattering using the SFC model. The overall tendency of J_R is to decrease with increasing energy. However, it is interesting to state that our J_R values agree well either with those obtained by Refs. [6,8] or those recently resulted from analysis of the same sets of data using microscopic

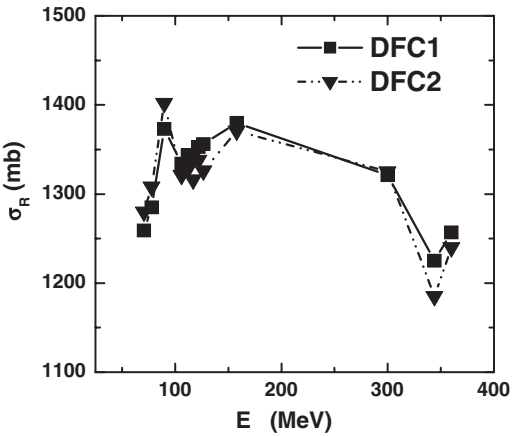

FIG. 5. Energy dependence of the total reaction cross sections deduced from the analysis of ^{12}C+^{12}C elastic scattering using the DFC1 and DFC2 potentials. Lines are drawn to guide the eyes.

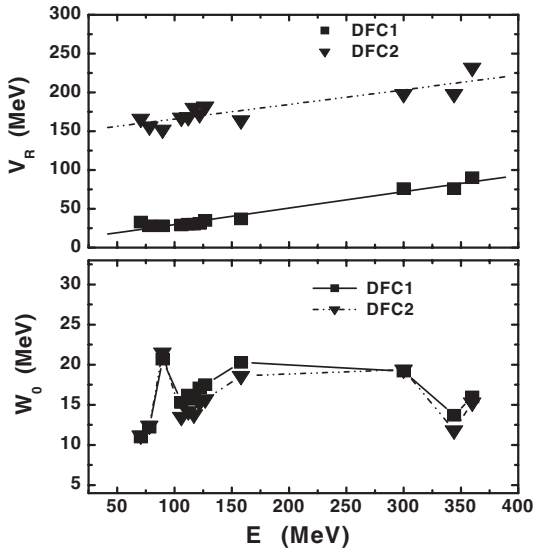

FIG. 6. Energy dependence of the real repulsive depth of the α-α interaction in the DFC1 and DFC2 potentials, straight lines are the least-square fits (upper part). Energy dependence the depth of the imaginary WS potential, lines are drawn to guide the eyes (lower part).

potentials based upon the JLM and SBM effective NN interactions [28].

The energy dependences of the obtained imaginary volume integrals, J_I, of both of the imaginary potentials supplemented with the DFC1 and DFC2 potentials, as shown in Fig. 4, are almost identical all over the investigated energy range. This behavior is attributed to the consistent values of the imaginary depth, W_0, used with both potentials, as shown in Table II. In Fig. 5 the energy dependence of the reaction cross section, σ_R, is shown. It is clear that the variations of σ_R, W_0 and J_I with energy are very similar, where σ_R determines the absorption produced by the imaginary potential. Comparing our values for σ_R with those obtained by the previous studies, we find that the obtained σ_R are consistent with those obtained by using microscopic potentials based upon the DDM3Y, BDM3Y [6], JLM and SBM [28] interactions.

For completeness, we display in Fig. 6 the energy dependence of both of the best-fit parameters, V_R and W_0. We note that the real repulsive part of α-α effective interaction, V_R, reveals slight linear energy dependence, where V_R increases as energy increases for both DFC1 and DFC2 potentials. We find $V_R = C + DE$, where $C = 8.6(146.8)$ MeV and $D = 0.21(0.19)$ for the DFC1 (DFC2) potential, i.e., the two dependences have similar slopes ($\sim$0.2). The depth of the imaginary part potential, W_0, does not show a clear behavior with energy. However, it is noticeable that, the imaginary potentials used in the present study are significantly shallower than those used by Abdullah *et al.*, for the analysis of ^{16}O+^{12}C elastic scattering.

V. CONCLUSIONS

In the present study, two types of the real double folding cluster optical potential, DFC1 and DFC2, for the ^{12}C+^{12}C system have been generated. In the first, the cluster structure

$^{12}C \equiv 3\alpha$ is considered. Then, the DFC1 potential is calculated with the total contribution from the α-α attractive and repulsive effective interactions folded with the α-cluster density distribution inside projectile and target nuclei. However, in the other type, the cluster structure $^{12}C \equiv A_\alpha\alpha + A_N N$ is taken into account and the DFC2 potential is calculated from contributions of the α-α attractive and repulsive interactions besides the α-N and NN interactions, folded with the α-like cluster and unclustered nucleon density distributions in the colliding nuclei. A phenomenological WS volume shape with a significant shallow depth has been considered for the imaginary part of the optical model potential.

Twelve sets of $^{12}C+^{12}C$ elastic scattering data in the energy range 70–360 MeV are analyzed using the derived potentials. Obtained results showed that successful description of the data all over the measured angular ranges can be obtained using the constructed semimicroscopic potentials. The success of our DFC1 and DFC2 potentials to reproduce the data is equivalent to that gained using microscopic potentials based upon the DDM3Y and BDM3Y effective NN interactions. However, from the present analysis, it has been noticed that, for high energy incident ^{12}C projectiles, the full α-clustering treatment ($^{12}C \equiv 3\alpha$) seams to be more successful to reproduce the data than the partial α-clustering concept ($^{12}C \equiv A_\alpha\alpha + A_N N$) and reversed behavior is observable at low energies.

The extracted reaction cross sections are quite consistent with those obtained by the previous studies by using microscopic potentials based upon the different versions of effective NN interactions.

Finally, despite the evident success of our model to describe $^{12}C+^{12}C$ elastic scattering data over the considered energy range, we recommend more studies to be performed on other kinds of HI reactions in order to confirm the validity of this model. In this connection, we draw attention to further aspects to be investigated in the future. Aside from the usual idiosyncracies of individual data sets, there are other sources of uncertainty in the analyses, such as choices of the folding ingredients, i.e., density distributions and effective interactions.

[1] P. E. Hodgson, *Nuclear Heavy-Ion Reactions* (Clarendon Press, Oxford, 1978).

[2] R. Bass, *Nuclear Reactions with Heavy Ions* (Springer-Verlag, Berlin, 1980).

[3] G. R. Satchler, *Direct Nuclear Reactions* (Clarendon Press, Oxford, 1983).

[4] A. M. Kobos, B. A. Brown, P. E. Hodgson, G. R. Satchler, and A. Budxanowski, Nucl. Phys. **A384**, 65 (1982); A. M. Kobos, B. A. Brown, P. E. Hodgson, R. Lindsay, and G. R. Satchler, *ibid.* **A425**, 205 (1984).

[5] M. El-Azab Farid and G. R. Satchler, Nucl. Phys. **A438**, 525 (1985); **A441**, 157 (1985).

[6] D. T. Khoa, W. von Oertzen, and H. G. Bohlen, Phys. Rev. C **49**, 1652 (1994); D. T. Khoa, W. von Oertzen, H. G. Bohlen, G. Bartnitzky, H. Clement, Y. Sugiyama, B. Gebauer, A. N. Ostrowski, T. Wilpert, M. Wilpert, and C. Langner, Phys. Rev. Lett. **74**, 34 (1995).

[7] M. El-Azab Farid and M. A. Hassanain, Nucl. Phys. **A678**, 39 (2000); **A697**, 183 (2002); Eur. Phys. J. A **19**, 231 (2004).

[8] M. El-Azab Farid, Z. M. M. Mahmoud, and G. S. Hassan, Nucl. Phys. **A691**, 671 (2001); Phys. Rev. C **64**, 014310 (2001).

[9] M. El-Azab Farid, Phys. Rev. C **65**, 067303 (2002); **74**, 064616 (2006).

[10] M. Karakoc and I. Boztosun, Phys. Rev. C **73**, 047601 (2006); Int. J. Mod. Phys. E **15**, 1317 (2006).

[11] M. N. A. Abdullah, S. Hossain, M. S. I. Sarker, S. K. Das, A. S. B. Tariq, M. A. Uddin, A. K. Basak, S. Ali, H. M. Sen Gupta, and F. B. Malik, Eur. Phys. J. A **18**, 65 (2003).

[12] M. N. A. Abdullah, M. S. I. Sarker, S. Hossain, S. K. Das, A. S. B. Tariq, M. A. Uddin, M. A. Uddin, A. S. Mondal, A. K. Basak, S. Ali, H. M. Sen Gupta, and F. B. Malik, Phys. Lett. **B571**, 45 (2003).

[13] S. Hossain, M. N. A. Abdullah, K. M. Hasan, M. Asaduzzaman, M. A. R. Akanda, S. K. Das, A. S. B. Tariq, M. A. Uddin, A. K. Basak, S. Ali, and F. B. Malik, Phys. Lett. **B636**, 248 (2006).

[14] G. R. Satchler and W. G. Love, Phys. Rep. **55**, 183 (1979).

[15] M. E. Brandan and G. R. Satchler, Phys. Rep. **285**, 143 (1997).

[16] A. J. Cole, W. D. M. Rae, M. E. Brandan, A. Dacal, B. G. Harvey, R. Legrain, M. J. Murphy, and R. G. Stokstad, Phys. Rev. Lett. **47**, 1705 (1981).

[17] H. G. Bohlen, X. S. Chen, J. G. Cramer, P. Frobrich, B. Gebauer, H. Lettau, A. Miczaika, W. von Oertzen, R. Ulrich, and T. Wilpert, Z. Phys. A **322**, 241 (1985).

[18] E. Stiliaris, H. G. Bohlen, P. Frobrich, B. Gebaur, D. Kolbert, W. von Oertzen, M. Wilpert, and Th. Wilpert, Phys. Lett. **B223**, 291 (1989).

[19] G. Bertsch, J. Borysowicz, H. McManus, and W. G. Love, Nucl. Phys. **A284**, 399 (1977).

[20] S. Ali and A. R. Bodmer, Nucl. Phys. **80**, 99 (1966); B. Buck, H. Friedrich, and C. Wheatley, Nucl. Phys. **A275**, 246 (1977).

[21] S. Sack, L. C. Biedenharn, and G. Breit, Phys. Rev. **93**, 321 (1954).

[22] O. M. Knyakov and E. F. Hefter, Z. Phys. A **301**, 277 (1981).

[23] Z. M. M. Mahmoud, M.Sc. thesis, Assiut University, 2000 (unpublished).

[24] E. V. Inopin and B. I. Tishchenko, Sov. Phys. JETP **11**, 840 (1960).

[25] J. F. Germond and C. Wilkin, Nucl. Phys. **A237** 477 (1975).

[26] N. M. Clarke, 1994 (unpublished).

[27] R. G. Stokstad, R. M. Wieland, G. R. Satchler, C. B. Fulmer, D. C. Hensley, S. Raman, L. D. Rickertsen, A. H. Snell, and P. M. Stelson, Phys. Rev. C **20**, 655 (1979).

[28] M. A. Z. Khalifa, Ph.D. thesis, South-Valley University, Egypt, 2006 (unpublished).